# Water Bound in Elytra of the Weevil *Liparus glabrirostris* (Küster, 1849) by NMR and Sorption Isotherm (Coleoptera: Curculionidae)

H. Harańczyk[a,*], M. Florek[a], P. Nowak[a] and S. Knutelski[b]

[a]Institute of Physics, Jagiellonian University, Cracow, Poland

[b]Institute of Zoology, Jagiellonian University, Cracow, Poland

Scanning electron microscopy micrograms of the elytra of *Liparus glabrirostris* showed a different dorsal and ventral surface and a multilayered inner structure. Hydration kinetics, sorption isotherm, and proton free induction decays are measured for hydrated elytra of the weevil species *Liparus glabrirostris* (Coleoptera: Curculionidae) in the atmosphere with controlled humidity. Very tightly bound water fraction with the mass $\Delta m/m_0 = 0.037 \pm 0.004$, and very short hydration time, tightly bound water $\Delta m/m_0 = 0.034 \pm 0.009$, and hydration time $t_1^{\rm h} = (3.31 \pm 0.93)$ h, and finally loosely bound water fraction with $t_2^{\rm h} = (25.5 \pm 7.8)$ h were distinguished. The sorption isotherm is sigmoidal in form, with the mass of water saturating primary water binding sites equal of $\Delta M/m_0 = 0.036$. The proton free induction decays show the presence of solid signal (well fitted by a Gaussian function) from elytra ($T_{2G}^* \approx 18$ $\mu$s), the immobilized water fraction ($T_{2L_1}^* \approx 120$ $\mu$s) and mobile water pool ($T_{2L_2}^* \approx 300$ $\mu$s). The hydration dependence of the water bound in elytra of *L. glabrirostris*, $L/S$ is linear showing the absence of water-soluble solid fraction and negligible content of water pool "sealed" in pores of the structure.

PACS: 82.56.Na

## 1. Introduction

Some insects are able to survive extremely deep dehydration. For instance, the lowest hydration level ever measured, was that of larvae of the African chironomid fly *Polypedilum vanderplanki* in their cryptobiotic form [1–5]. During cryptobiosis *P. vanderplanki* can survive either extremely low or extremely high temperatures and irradiation [6–8].

Imagines of several beetle species differ in their resistance to acute water stress, e.g. ground beetles are much less resisted than weevils and darkling beetles [9]. Some species of East African ground beetles and weevils developed of a closed subelytral cavity allowing them better control of the amount of breathed out water vapor which combined with the decrease in cuticular water permeability and lowered metabolic rate helps them to survive during very dry period [10]. The desiccation resistance depends also on body size [11].

The freezing tolerance stimulates desiccation tolerance for such extremophilic organisms as lichens [12–17] and insects [9, 18], and indeed, desiccation resistant weevils are among the species populating Maritime Antarctics [19, 20].

Insect cuticle plays important role in controlling water level in the insect body [21], which focused our attention on water behavior in elytra of European weevil species *Liparus glabrirostris* Küster, 1849 representing the family Curculionidae. These species populate mainly mountain and submountain areas of central Europe between the Pyrenees Mountains and Transylvania region in Carpathians. We analyzed a number and a distribution of water binding sites, sequence and kinetics of their saturation, and the formation of tightly and loosely bound water fractions at different steps of hydration process.

## 2. Materials and methods

Beetles of *Liparus glabrirostris* were collected in spring from the area of the Gorce Mountains (Western Carpathians, southern Poland). The elytra dissected from dead specimens, and then dried at room temperature ($t = 22\,°C$). The elytron is prolate in form, with the average thickness of $(170 \pm 19)$ $\mu$m. Close to anterior and to posterior margins the thickness slightly increases (up to *ca.* 200 $\mu$m). The overall surface equals *ca.* 56 mm$^2$; the density 1.2 g/cm$^3$, and the surface-to-mass ratio 44 cm$^2$/g.

Detailed examination of the structure of elytra of *Liparus glabrirostris* were made using a scanning electron microscope (SEM). Different samples of the dried elytra were coated in graphite and detected at different magnification level.

The hydration level of the air dry elytra was equal to $\Delta m/m_0 = 0.055 \pm 0.004$. Before the hydration courses the elytra samples were incubated over silica gel ($p/p_0 = 0\%$), reaching the hydration level equal to $\Delta m/m_0 = 0.037 \pm 0.004$. Before placing in NMR tubes the samples of elytra were split into prolate fragments 2–3 mm wide.

The hydration time-courses were performed in the atmosphere with controlled humidity, at room temperature

* corresponding author; e-mail: hubert.haranczyk@uj.edu.pl

($t = 22\,°C$), over the surface of $H_3PO_4$ ($p/p_0 = 9\%$ supersaturated solutions of $CH_3COOK$ ($p/p_0 = 23\%$), $CaCl_2$ ($p/p_0 = 32\%$), $K_2CO_3$ ($p/p_0 = 44\%$), $Na_2Cr_2O_7$ ($p/p_0 = 52\%$), $NH_4NO_3$ ($p/p_0 = 63\%$), $Na_2S_2O_3$ (76%), $K_2CrO_3$ (88%), $Na_2SO_4$ (93%), $K_2SO_4$ ($p/p_0 = 97\%$), and over the water surface ($p/p_0 = 100\%$).

The dry mass of the elytra was determined after heating at $70\,°C$ for 72 h. Higher temperatures were not used to avoid the decomposition of some organic constituents of the sample [22].

Proton spectra were recorded on a Bruker Avance III spectrometer (Bruker Biospin), operating at the resonance frequency 300 MHz (at $B_0 = 7$ T), with the transmitter power used equal to 400 W. The pulse length was $\pi/2 = 1.5\ \mu$s, bandwidths was 300 kHz, and repetition time was 2 s.

Proton free induction decays (FIDs) were obtained using WNS HB-65 high power relaxometer (Waterloo NMR Spectrometers, St. Agatha, Ontario, Canada). The resonance frequency was 30 MHz (at $B_0 = 0.7$ T); the transmitter power was 400 W; and the pulse length $\pi/2 = 1.25\ \mu$s. FIDs were acquired using Compuscope 2000 card of an IBM clone controlling the spectrometer and averaged over 1000 accumulations. Repetition time was 2.003 s.

The obtained data were analyzed using the FID analyzing procedure of a two-dimensional (in time domain) NMR signal-analyzing program CracSpin written at the Jagiellonian University, Cracow [23] or by commercially available program Origin 7.0.

## 3. Results

### 3.1. SEM micrograms

Electron micrograms of *Liparus glabrirostris* elytra reveal a very composed inner structure. Dorsal surfaces show the appearance of hair-like elongated structures (*ca.* 300 $\mu$m long, *ca.* 20 $\mu$m in diameter) gathered in isolated areas (Fig. 1). Higher magnification presents that the surface is organized in flat hexagons (125–145 $\mu$m in diameter) (Fig. 1b and c). From the centers of hexagons there often start the elongated structures, however, in the gatherings their density is significantly higher. Ventral sides are regularly covered by the conical denticles (*ca.* 10 $\mu$m long, *ca.* 5 $\mu$m in diameter).

The coverage density equals $42000/\text{mm}^2$ (Fig. 2). Perpendicular cross-sections show the multilayered inner structure of elytron. The thickness of the layer equals $3.77 \pm 1.68\ \mu$m (Fig. 3d). In terminal areas of elytron the cylindrical holes (diameter 10 $\mu$m) are observed (Fig. 3a) which are surrounded by whirled layers. The layers on the outer side of the pipe are thicker $4.23 \pm 0.52\ \mu$m, whereas those localized closer to the ventral side of elytron are significantly thinner $2.03 \pm 0.33\ \mu$m (Fig. 3a). The parallel cross-sections reveal flat layers consist of column-like elements which are directed in different angles; also, they are separated by the layer of columns placed perpendicularly to the elytron surface, which strengthens the elytron surface (Fig. 4).
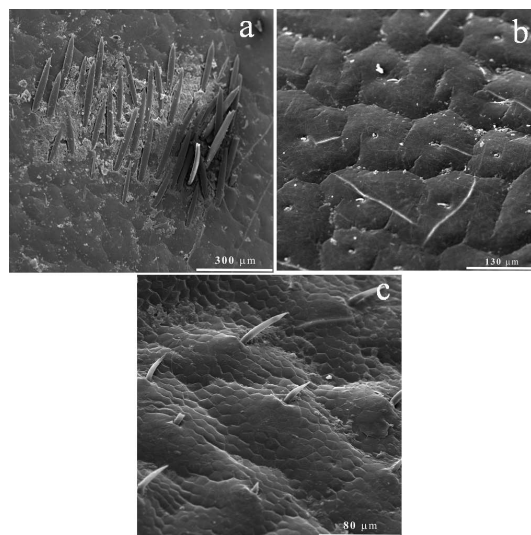


Fig. 1. Dorsal side of the surface of the elytra of *Liparus glabrirostris* in different magnifications: (a) scale division 300 $\mu$m bar, (b) 130 $\mu$m, and (c) 80 $\mu$m.
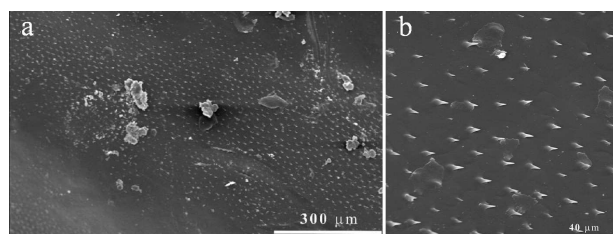


Fig. 2. Ventral side of some parts of the surface of the elytra of *Liparus glabrirostris* in different magnifications (a) scale division 300 $\mu$m bar, and (b) 40 $\mu$m.

### 3.2. Hydration kinetics and sorption isotherm

The hydration courses for *Liparus glabrirostris* elytra were performed in the atmosphere with the controlled humidity. For the relative humidities, $p/p_0$, between 9% and 52%, the mass of water bound to the elytra surfaces is fitted well by a single exponential function (see Fig. 5)

$$\Delta m/m_0 = A_0^{\text{h}} + A_1^{\text{h}}\left[1 - \exp(-t/t_1^{\text{h}})\right], \qquad (1a)$$

where $\Delta m/m_0$ is the relative mass increase expressed in units of dry mass, $m_0$, $A_1^{\text{h}}$ is the saturation level for the fast component solely observed at given relative humidity range, and $A_0^{\text{h}}$ is the hydration level at $p/p_0 = 0\%$ (very tightly bound water fraction).

At relative humidity 44% and higher the slow hydration component appeared and the hydration courses were fitted well by the two-exponential function (Fig. 5):

$$\Delta m/m_0 = A_0^{\text{h}} + A_1^{\text{h}}\left[1 - \exp(-t/t_1^{\text{h}})\right]$$
$$+ A_2^{\text{h}}\left[1 - \exp(-t/t_2^{\text{h}})\right], \qquad (1b)$$

where $A_0^{\text{h}}$ is the saturation level of very tightly bound water fraction (at $p/p_0 = 0\%$), $A_1^{\text{h}}$ and $A_2^{\text{h}}$ are the saturation hydration levels for a fast and slow component,
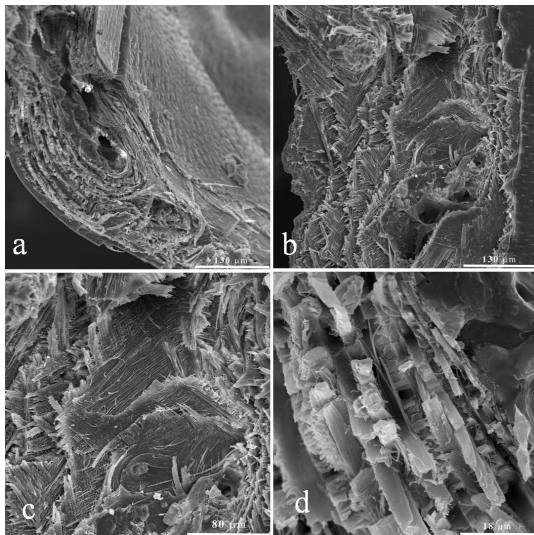
Fig. 3. Perpendicular cross-section of the elytra of *Liparus glabrirostris* at different magnification: (a) whirling of layers, scale division 130 $\mu$m, (b) crossing of fibers in subsequent layers, scale division 130 $\mu$m, (c) distorted layers, scale division 80 $\mu$m, and (d) view of the layers 18 $\mu$m.
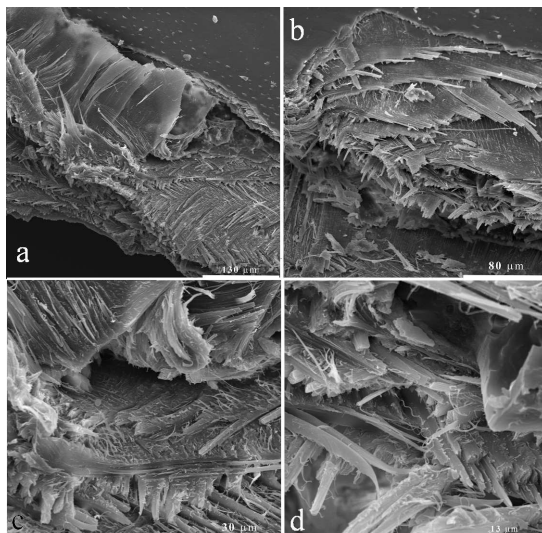


Fig. 4. Parallel cross-section of the elytra of *Liparus glabrirostris* at different magnification: (a) short columns perpendicular to the elytra surface, scale division 130 $\mu$m, (b) crossing of fibers in subsequent layers, scale division 80 $\mu$m, (c) layers split into fiber-like elements, scale division 30 $\mu$m, and (d) fiber-like elements in magnification, scale division 13 $\mu$m.

and $t_1^h$ and $t_2^h$ are hydration times for a fast and slow component (tightly and loosely bound water fraction), respectively.

The mass of the very tightly bound water expressed in units of dry mass equals $A_0^h = 0.037 \pm 0.004$, with the hydration time shorter than 10 min, which was the first
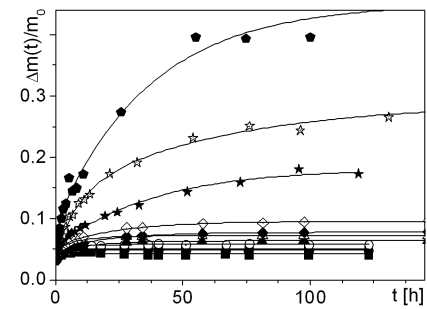


Fig. 5. The hydration kinetics for elytra of *Liparus glabrirostris* Küster, 1849 performed from the gaseous phase at different values of relative humidity $p/p_0$, recorded as relative mass increase expressed in units of dry mass $\Delta m/m_0$. Targets humidity: $p/p_0 = 9\%$ — close squares, $p/p_0 = 23\%$ — open squares, $p/p_0 = 32\%$ — close circles, $p/p_0 = 44\%$ — open circles, $p/p_0 = 52\%$ — close triangles, $p/p_0 = 63\%$ — open triangles, $p/p_0 = 76\%$ — close diamonds, $p/p_0 = 88\%$ — open diamonds, $p/p_0 = 93\%$ — close starlets, $p/p_0 = 97\%$ — open starlets, $p/p_0 = 100\%$ — close pentagons. The error bars are within the plot symbols.

sampling point. Tightly bound water is characterized by a mass $A_1^h = 0.034 \pm 0.009$, and hydration time $t_1^h = 3.31 \pm 0.93$ h. The mass of loosely bound water fraction gradually increases with increasing relative humidity, and hydration time equals $t_2^h = 25.5 \pm 7.8$ h.
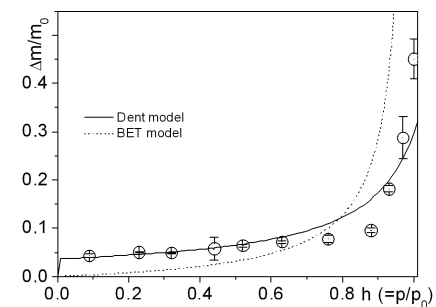


Fig. 6. The sorption isotherm for elytra of *Liparus glabrirostris*. The values of $h$ (= $p/p_0$) representing the relative humidity and the values of relative mass increase, $\Delta m/m_0$, are defined as the $C^h$ values are taken from Eq. (1).

The total saturation hydration level $C^h$ calculated as a sum of saturation hydrations for all water fractions detected in hydration kinetics was taken to construct the sorption isotherm

$$C^h = A_0^h + A_1^h + A_2^h. \tag{2}$$

The sorption isotherm for *L. glabrirostris* elytra is approximately sigmoidal in form (Fig. 6), and is significantly better fitted using the Dent model [24] (Eq. (3)) than using the Brunauer–Emmett–Teller (BET) model [25]:

$$C^{h}(h) = \frac{\Delta M}{m_0} \frac{b_1 h}{(1-bh)(1+b_1 h - bh)}, \qquad (3)$$

where $h = p/p_0$ is relative humidity expressed as a ratio, $\Delta M/m_0$ is the mass of water saturating primary water binding sites; the parameter $b$ is a coverage of the $n$-th water layer expressed in units of the coverage of $(n-1)$-th: $S_n/S_{n-1}|_{h=1} = b$, where $S_i$ is the population of $i$-th water layer, and the contribution of empty primary binding sites at $h = 1$ is expressed by the reciprocal of $b_1$: $S_0/N|_{h=1} = 1/b_1$, where $S_0$ is the number of water binding sites on the surface.

The mass of water saturating primary water binding sites equals $\Delta M/m_0 = 0.036$, which is close to the mass of very tightly bound water detected in hydration kinetics. The parameter $b$ simulating the form of water droplets bound on the surfaces equals $b = 0.865$, and the proportion of primary binding sites unoccupied at $h = 1$ is very small, $1/b_1 < 0.01\%$.

### 3.3. NMR measurements in time domain

Proton FIDs, performed at room temperature for *Liparus glabrirostris* elytra are superposition of solid component, well fitted by Gaussian function and one exponentially relaxing liquid component. For the hydration level exceeding $\Delta m/m_0 > 0.15$, a second exponentially relaxing component coming from loosely bound water fraction was detected (Eq. (4)). In general, FID is given by

$$\mathrm{FID}(t) = S \exp\left(-\left(\frac{t}{T_{2S}^*}\right)^2\right) + L_1 \exp\left(-\frac{t}{T_{2L_1}^*}\right)$$
$$+ L_2 \exp\left(-\frac{t}{T_{SL_2}^*}\right), \qquad (4)$$

where $S$ is the amplitude and $T_{2S}^*$ is proton relaxation time (taken for $1/e$-value of Gaussian) of the solid signal component; and $L_1$ and $L_2$ are the amplitudes, and $T_{2L_1}^*$ and $T_{2L_2}^*$ are the relaxation times of both proton liquid fractions, respectively.

The solid component of the recorded FID function does not reveal the "beat" pattern, which is characteristic for the Abragam function [26, 27]. The moment expansion of solid signal [26]:

$$S(t) = S\left(1 - \frac{M_2}{2!}t^2 + \frac{M_4}{4!}t^4 - \frac{M_6}{6!}t^6 + \dots\right) \qquad (5)$$

gives $M_4/M_2^2 = 2.40$, close to the value expected for Gaussian ($M_4/M_2^2 = 3$). Thus, the solid component of FID signal may be sufficiently well approximated by the Gaussian function. The relaxation time for solid component equals $T_{2S}^* \approx 20$ $\mu$s (Fig. 7), which is characteristic for solid matrices of many dry biological systems [28].

The observed liquid signal fractions come from water fraction differentiated by their mobility, and thus by their binding and/or proximity to the elytra surfaces. The $T_{2L_1}^* \approx 100$ $\mu$s (Fig. 7) of the $L_1$ component is characteristic for tightly bound water in several biological systems, e.g. lichen thalli [13–17], as well as of many other ones
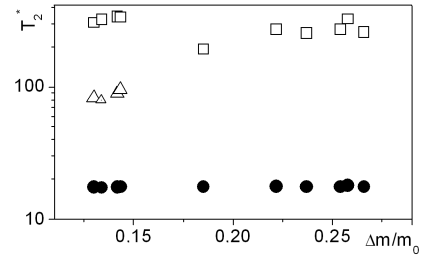


Fig. 7. The hydration dependence of proton relaxation times measured from FID for the elytra of *Liparus glabrirostris*. Solid Gaussian component ($S$) — close circles, tightly bound water/component ($L_1$) — open triangles, and loosely bound water fraction ($L_2$) — open squares.

([12] and the references therein). The $L_2$ signal with $T_{2L_2}^* \approx 560$ $\mu$s, shortened by $B_0$ inhomogeneities, comes from water loosely bound on elytra surface and for higher hydration level from free water fraction [29].
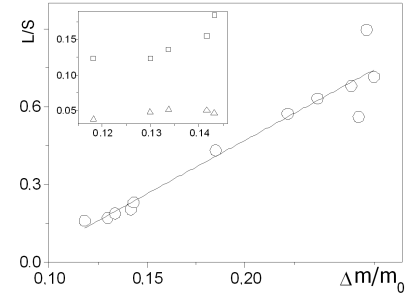


Fig. 8. The total liquid signal, $(L_1 + L_2)/S$, expressed in units of solid signal hydration dependence for the elytra of *Liparus glabrirostris* (open circles). Inset shows the tightly bound water (open triangles) and loosely bound water (open squares) signal hydration dependence. The solid line was calculated from Eq. (6).

The solid signal component relaxation time $T_{2S}^*$ is only slightly changed with the hydration level (see Fig. 8), which means that solid matrix of the elytra structure does not change for $\Delta m/m_0 < 0.27$. Thus, the liquid signal component may be expressed in units of solid, $L/S$ (Fig. 8). The hydration dependence of total liquid signal is well fitted by a linear function

$$(L_1 + L_2)/S = -(0.360 \pm 0.076)$$
$$+ (4.15 \pm 0.37)\Delta m/m_0. \qquad (6)$$

The linear form of the total liquid signal hydration dependence shows the absence of water soluble solid fraction [15–17, 30].

Figure 9 shows proton NMR spectrum recorded at room temperature for elytra of *L. glabrirostris* hydrated to $\Delta m/m_0 = 0.0775$. The line is composed of the broad solid component coming from the solid matrix of elytra and the narrow component coming from wa-
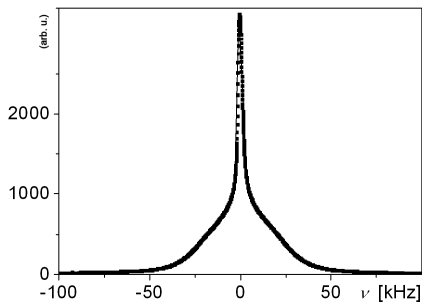
Fig. 9. Proton NMR spectrum for the elytra of *Liparus glabrirostris* recorded at 300 MHz; the pulse length $\pi/2 = 1.5$ $\mu$s. The relative mass increase was $\Delta m/m_0 = 0.0775$.

ter bound in *L. glabrirostris* elytra. The obtained spectrum is well fitted by a superposition of Gaussian component [$\Delta\nu_G = (44.29 \pm 0.04)$ kHz] and two narrow lines fitted by Lorentzian functions coming from water tightly and water loosely bound in pores of elytra [$\Delta\nu_{L_1} = (3.51 \pm 0.46)$ kHz, the value averaged for hydration levels between $\Delta m/m_0 = 0.05$ and 0.075], and $\Delta\nu_{L_2} = (1.42 \pm 0.11)$ kHz, respectively [see Eq. (7)]:

$$A(\nu) = \frac{A_S}{\Delta\nu_G\sqrt{\pi/2}}\exp\left(-2\ln 4 \times \left(\frac{(\nu - \nu_G)}{\Delta\nu_G}\right)^2\right)$$

$$+ \frac{2A_{L_1}}{\pi}\left[\frac{\Delta\nu_{L_1}}{4(\nu - \nu_{L_1})^2 + \Delta\nu_{L_1}^2} + \ldots\right]$$

$$\ldots + \frac{2A_{L_2}}{\pi}\left[\frac{\Delta\nu_{L_2}}{4(\nu - \nu_{L_2})^2 + \Delta\nu_{L_2}^2}\right], \quad (7)$$

where $\nu_G$, $\nu_{L_1}$, and $\nu_{L_2}$ are Gaussian and Lorentzian peak positions, respectively; and finally $A_S$, $A_{L_1}$, and $A_{L_2}$ are the amplitudes of the Gaussian and Lorentzian peaks, respectively.
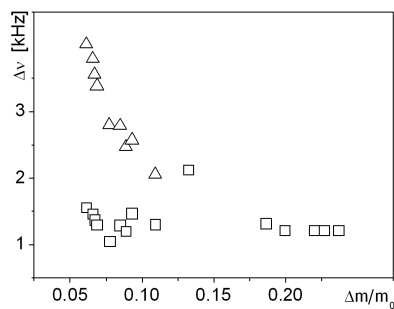


Fig. 10. The halfwidths of Lorentzian line components of $^1$H-NMR line for the elytra of *Liparus glabrirostris* ($\Delta\nu_{L_1}$ — open triangles, $\Delta\nu_{L_2}$ — open squares).

The halfwidth of Lorentzian line, $\nu_{L_1}$, coming from tightly bound water fraction decreases with increasing hydration level (Fig. 10), which suggests the increas-

ing mobility of that water fraction or proton fast exchange between tightly bound water and loosely bound water at some areas of the structure. For hydration level $\Delta m/m_0 > 0.1$ the signal coming from tightly bound water is no longer fitted for numerical reasons (Fig. 10).
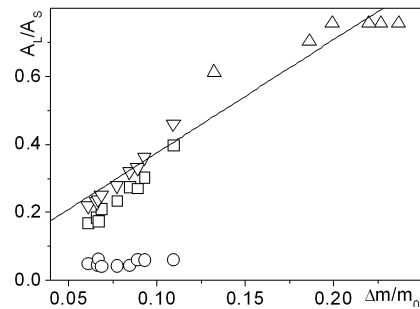


Fig. 11. The hydration dependence of the area under Lorentzian, liquid, line component expressed in units of Gaussian, solid, line component [triangles = total liquid signal $(A_{L_1} + A_{L_2})/A_S$; open squares = tightly bound water signal, $A_{L_1}/A_S$; and open circles = $A_{L_2}/A_S$] for the elytra of *Liparus glabrirostris*. The solid line was calculated from Eq. (8).

The total liquid signal expressed in units of solid is well fitted by the linear dependence (Fig. 11) according to

$$(A_{L_1} + A_{L_2})/A_S = (0.042 \pm 0.027)$$
$$+ (3.33 \pm 0.19)\Delta m/m_0. \quad (8)$$

Tightly bound water signal intensity, $A_{L_1}$, does not change with the increased hydration level, whereas loosely bound water increases linearly with increased hydration level (Fig. 11). This confirms the hypothesis that both bound water fractions are differentiated by the proximity to the surfaces of the solid matrix of elytra.

## 4. Discussion

The composed structure of the elytra of *Liparus glabrirostris* (Figs. 1–4) allows water vapor penetration of the pores and subsequent deposition of water molecules. The hydration level reached in $p/p_0 = 100\%$ is quite high, and equals $\Delta m/m_0 = 0.4$. Three fractions of bound water were detected: very tightly bound water, tightly bound water fraction, and loosely bound water fraction, which were differentiated by the proximity to the surfaces of elytron.

The water soluble solid fraction is not detected in *L. glabrirostris* elytra. It is recorded at initial phases of hydration in lichen thalli, where such a fraction is consisted of polyols and sugars [15–17, 31]; in horse chestnut bast, it is mainly sucrose [30]. In *L. glabrirostris* simple sugars and polyols were absent in pores of the elytra structure. On the other hand, the presence of the "sealed" water pool in closed pores of the elytra matrix is possible [32, 33]. The value of the slope of the $L/S$ hydration dependence suggest the presence of paramagnetic ions in solid matrix of elytra [34].

Sorption isotherm yields the mass of water saturating primary water binding sites. Assuming that water bound to primary water binding sites forms continuous monolayer one may estimate the total inner surface of *L. glabrirostris* defined as water-accessible surface [12]. Thus, the obtained total water-accessible surface equals of 107.5 m$^2$/g of dry mass. The analysis of electron micrograms gives that the number of layers inside elytron varies between 80 (extremely thin layers in the vicinity of pipes) (Fig. 3a) down to 45 (average value for the central part of elytron). The micrograms of dorsal and ventral side show that the present structure do not very much increase the value of surface. Thus, the total surface of all layer surfaces varies between 0.40 and 0.73 m$^2$/g. This means that vast majority of primary water sorption takes part inside the inner layers of *L. glabrirostris* elytron.

## Acknowledgments

## References

[1] H.E. Hinton, *Proc. Zool. Soc. Lond.* **121**, 371 (1951).

[2] H.E. Hinton, *J. Insect Physiol.* **5**, 286 (1960).

[3] H.E. Hinton, *Nature* **188**, 336 (1960).

[4] H.E. Hinton, *J. Insect Physiol.* **5**, 286 (1960).

[5] H.E. Hinton, *Proc. R. Soc. B* **171**, 43 (1968).

[6] M. Watanabe, T. Kikawada, N. Minagawa, F. Yukuhiro, T. Okuda, *J. Exp. Biol.* **205**, 2799 (2002).

[7] M. Watanabe, T. Kikawada, T. Okuda, *J. Exp. Biol.* **206**, 2281 (2003).

[8] M. Watanabe, T. Sakashita, A. Fujita, T. Kikawada, D.D. Horikawa, Y. Nakahara, S. Wada, T. Funayama, N. Hamada, Y. Kobayashi, T. Okuda, *Int. J. Radiat. Biol.* **82**, 587 (2006).

[9] R.A. Ring, W. Block, L. Sømme, M.R. Worland, *Polar Biol.* **10**, 581 (1990).

[10] K.E. Zachariassen, J. Andersen, M.O. Maloiy, M.Z. Kamau, *Comp. Biochem. Physiol. A* **86**, 403 (1987).

[11] M.D. Le Lagadec, S.L. Chown, C.H. Scholtz, *J. Comp. Physiol. B* **168**, 112 (1998).

[12] H. Harańczyk, *On Water in Extremely Dry Biological Systems*, WUJ, Kraków 2003.

[13] H. Harańczyk, S. Gaździński, M.A. Olech, *New Phytol.* **138**, 191 (1998).

[14] H. Harańczyk, S. Gaździński, M.A. Olech, *New Aspects in Cryptogamic Research, Contribution in Honour of Ludger Kappen. Bibl. Lichenol.* **75**, 265 (2000).

[15] H. Harańczyk, A. Pietrzyk, A. Leja, M. Olech, *Acta Phys. Pol. A* **109**, 411 (2006).

[16] H. Harańczyk, M. Bacior, M.A. Olech, *Antarct. Sci.* **20**, 527 (2008).

[17] H. Harańczyk, M. Bacior, P. Jastrzębska, M.A. Olech, *Acta Phys. Pol. A* **115**, 516 (2009).

[18] M.R. Worland, W. Block, *J. Insect Physiol.* **49**, 193 (2003).

[19] M. van der Merve, S.L. Chown, V.R. Smith, *Polar Biol.* **18**, 331 (1997).

[20] S.L. Chown, M. van Drimmelen, *Polar Biol.* **12**, 527 (1992).

[21] J.F.V. Vincent, U.G.K. Wegst, *Arth. Struct. Dev.* **33**, 187 (2004).

[22] D.F. Gaff, *Oecologia (Berl.)*, **31**, 95 (1977).

[23] W. Węglarz, H. Harańczyk, *J. Phys. D, Appl. Phys.* **33**, 1909 (2000).

[24] R.W. Dent, *Text. Res. J.* **47**, 145 (1977).

[25] S. Brunauer, P.H. Emmett, E. Teller, *J. Am. Chem. Soc.* **60**, 309 (1938).

[26] A. Abragam, *The Principles of Nuclear Magnetism*, Clarendon Press, Oxford 1961.

[27] W. Derbyshire, M. Van Den Bosch, D. Van Dusschoten, W. MacNaughtan, I.A. Farhat, M.A. Hemminga, J.R. Mitchell, *J. Magn. Res.* **168**, 278 (2004).

[28] M.M. Pintar, *Magn. Reson. Imag.* **9**, 753 (1991).

[29] A. Timur, *J. Petroleum Technol.* **21**, 775 (1969).

[30] H. Harańczyk, W.P. Węglarz, S. Sojka, *Holzforschung* **53**, 299 (1999).

[31] N. Hamada, K. Okazaki, M. Shinozaki, *Bryologist* **97**, 176 (1994).

[32] H. Harańczyk, A. Leja, K. Strzałka, *Acta Phys. Pol. A* **109**, 389 (2006).

[33] H. Harańczyk, A. Leja, M. Jemioła-Rzemińska, K. Strzałka, *Acta Phys. Pol. A* **115**, 526 (2009).

[34] I. Horčičko, Š. Voráčová, *Acta Univ. Palacki. Olomouc. Fac. rer. nat. 1999, Biol.* **37**, 57 (1999).